Semnan University

Progress in Physics of Applied Materials

journal homepage: https://ppam.semnan.ac.ir/

Competition between Heisenberg and bond-dependent interactions driven an incommensurate ordering in honeycomb cobaltates

Maryam Ghafari-Mofrad [a], Hamid Mosadeq[a*], Mohammad-Hossein Zare[b]

[a] *Department of Physics, Faculty of Science, Shahrekord University, Shahrekord, Iran,*
[b] *Department of Physics, Qom University of Technology, Qom*

ARTICLE INFO

Article history:
Received: 2 January 2024
Revised: 17 February 2024
Accepted: 17 February 2024

Keywords:
Generalized Kitaev-Heisbenerg Model
Luttinger-Tiasza Method
Incommensurate Magnetic Phases

ABSTRACT

Experimental observations show that the zero-field ground state of honeycomb-layered cobaltates is an incommensurate spiral order with an ordering wave vector along the $\Gamma \rightarrow M$line. However, in the presence of a magnetic field, the incommensurate magnetic phase becomes unstable and the quantum spin liquid phase becomes stable in this class of materials. Here, the central question we address is how to realize the incommensurate order theoretically. For this purpose, we are interested in studying the generalized Kitaev-Heisbenerg model and investigating the interplay effect between conventional Heisenberg and bond-dependent exchange interactions on the stability of the incommensurate spiral order. Our results show that the interplay between the second neighbor Heisenberg interaction and bond-dependent exchange interactions play a vital role in the stability of incommensurate phases. The competition between the second nearest nearest-neighbor interaction and the off-diagonal bond-directional exchange for $BaCo_2(AsO_4)_2$ may place this material in proximity to a quantum spin liquid phase. The quantum spin liquid can be accessible for $BaCo_2(AsO_4)_2$ in the presence of an external magnetic field.

1. Introduction

Two-dimensional (2D) magnets without long-range order have blossomed into a rich area for investigation, which have been studied for many decades, starting by investigating the effects of disorder in spin glasses [1,2] and resonant valence coupling modes in frustrated magnetic materials [3,4]. 2D frustrated spin systems with $S = \frac{1}{2}$ have lately attracted great interest due to their potential for realizing the quantum spin liquid (QSL), a magnetically disordered state which respects all the symmetries of the systems, even at absolute zero temperature [4,5].

Aside from the fascinating physics of QSLs, according to the resonating valence bond theory of Anderson, QSLs are the parent state for high-temperature unconventional superconductors. Various quantum materials are proposed to host this nontrivial collective phase due to extreme quantum fluctuations where frustration induces a macroscopically-degenerate ground state at the classical level [6,7]. It should be noted that QSLs originating from geometrical frustration in triangular, kagome, and pyrochlore lattices or quantum spin models with frustration can generate a macroscopic ground state degeneracy, resulting in strong quantum fluctuations. These frustrations driven spin configurations behave as liquid and do not exhibit long-range magnetic order even at absolute zero temperature.

Honeycomb lattice Kitaev materials in which bond-dependent exchange interactions between spins induce strong quantum fluctuations and frustrate spin configurations. Kitaev-QSLs may exist in spin-orbit coupled Mott insulators due to the interplay between spin-orbit coupling and three-fold rotational symmetry of a honeycomb lattice giving rise to the bond dependent Ising-type interactions (Kitaev-type exchange interaction) between nearest-neighbors [8]. Most recent studies on the

* Corresponding author.
E-mail address: hamid.mosadegh@gmail.com

Cite this article as:
Ghafari-Mofrad, M., Mosadeqa H., Zare M.H., 2024. Competition between Heisenberg and bond-dependent interactions driven an incommensurate ordering in honeycomb cobaltates. *Progress in Physics of Applied Materials*, 4(1), pp.7-12.DOI: 10.22075/PPAM.2024.32866.1081

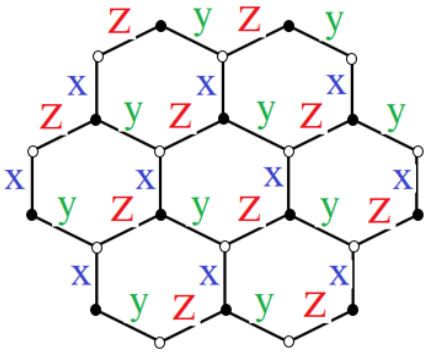

Fig. 1. (Color online) A sketch of a honeycomb lattice, which is composed of two triangular sublattices as denoted by white and black circles. Nearest-neighbor interactions labeled by the x, y, and z bonds.

Kitaev materials are devoted to $4d$ and $5d$ ions with large spin-orbit coupling such as Ru^{3+} and Ir^{4+} [9,10]. However, in this class of materials, due to relatively large non-Kitaev interactions, the magnetic ground state of these systems at low temperatures is different from the Kitaev spin liquid phase [11-17].

Recently, cobalt compounds with a honeycomb structure have received massive attention [18,19]. Theoretical studies show that the spin model of this class of materials consists of the bond-dependent Ising interactions on the honeycomb lattice [20,21]. The experimental observations report that its magnetic ground state is an incommensurate spiral order along the $\Gamma \to M$ high-symmetry within the first Brillouin zone (FBZ). Measurement of heat capacity, magnetization and also neutron scattering studies of Kitaev materials $3d^7$with a honeycomb structure such as $BaCo_2(AsO_4)_2(BCAO)$ [22,23] show that its magnetic ground state is an incommensurate spiral order along the $\Gamma \to M$ high-symmetry line of the FBZ [24].

Honeycomb-layered cobaltates $Ba_2Co_2(AsO_4)$ is promising new candidates to realize the Kitaev spin liquid state. The experimental observations report that its magnetic ground state is an incommensurate spiral order along $\Gamma \to M$ the high-symmetry line of the FBZ. Different experimental studies reported the pursuit of the QSL phase for a finite range of magnetic fields between low-field magnetic order and the high-field trivial state in the Kitaev honeycomb magnet $Ba_2Co_2(AsO_4)$ [24]. The search for the intermediate field-induced a gapped topological spin liquid in $Ba_2Co_2(AsO_4)$, that hosts free Majorana edge modes, by the promise of application of its excitations in topologically protected quantum computation [25-27].

The microscopic origin of the incommensurate spiral order in the BCAO remains unclear. In this paper, we are interested to map out the magnetic ground states of generalized Kitaev-Heisenberg model that are realized classically. To investigate the importance of the off-diagonal exchange interactions in describing the ground state of BCAO theoretically, we here use the Luttinger-Tisza (LT) analytical method [28,29].

2. Model and method

In the Kitaev materials such as BCAO with spin-orbit coupled pseudospin-1/2 degrees of freedom, we consider the generalized JKΓΓ′ model on a honeycomb lattice as [30,31]:

$$H = \sum_{n=1,2} \sum_{<ij>_n} J_n (S_i^x S_j^x + S_i^y S_j^y + S_i^z S_j^z)$$

$$+ \sum_{\gamma=x,y,z} \sum_{<ij>_\gamma} [K S_i^\gamma S_j^\gamma + \Gamma (S_i^\alpha S_j^\beta + S_i^\beta S_j^\alpha)] \quad (1)$$

here, J and K are the conventional Heisenberg and Kitaev interactions, respectively, while Γ and Γ′ are the symmetry-allowed off-diagonal exchange interaction. The first summation on n stands for the first and second Heisenberg exchange interactions. In addition, the summation on γ associated with the nearest-neighbor bonds on the honeycomb lattice with $\gamma \in \{x, y, z\}$ and S_i^γ is the γ-component of spin-$\frac{1}{2}$ operator at site i. On z bonds $(\alpha, \beta, \gamma) = (x, y, z)$ and for the x and y bonds obtained with cyclic permutation. The three bond types (x, y, z) are marked by three different labels in Figure 1. For the sake of simplicity, we here assume $J_1 = 1$.

The LT method is a way of finding the ground state of a classical quadratic Hamiltonian. By Fourier transformation of the spins and the couplings, one can find a matrix representation for a quadratic spin Hamiltonian in the Fourier space. To diagonalize the matrix representation of the quadratic spin Hamiltonian, Eq. (1), which is obtained by using Fourier transformations, give the stable magnetic configurations for the different constant couplings, as will be discussed in more details below. Note that we here imply the weak constrain, $\sum_i |s_i|^2$instead of the constraint of fixed spin length at each site. Here, N is the number of lattice points.

Honeycomb lattice is composed of the two triangular sub-lattices (Figure 1), therefore the Fourier transformations of the spins for each sublattice become as $\vec{S}_{l,\vec{R}_i} = \sqrt{2/N} \sum_{\vec{q}} e^{i\vec{q}\cdot\vec{R}_i} \vec{S}_{l,\vec{q}}$ with the sublattice index $l = A, B$. Here, $\vec{R}_i$ indicates the translational vectors of the triangular Bravais lattice and $\frac{N}{2}$ is the number of primitive cells. Substituting the above transformations into the classical Hamiltonian, Eq. (1), we can obtain the Hamiltonian in terms of the Fourier components as:

$$H = \sum_{\vec{q}} \Psi_{-\vec{q}}^T H_{\vec{q}} \Psi_{\vec{q}}$$

$$\text{with} \quad \Psi_{\vec{q}} = \begin{pmatrix} \vec{S}_{A\vec{q}} \\ \vec{S}_{B\vec{q}} \end{pmatrix} \quad (2)$$

where $\vec{q}$ belongs to the FBZ. The H_q matrix is defined as

$$H_{\vec{q}} = \begin{pmatrix} F_{\vec{q}} & G_{\vec{q}} \\ G_{\vec{q}}^\dagger & F_{\vec{q}} \end{pmatrix}$$

which

$$F_{\vec{q}} = \frac{J_2}{2} \begin{pmatrix} 1 & 0 & 0 \\ 0 & 1 & 0 \\ 0 & 0 & 1 \end{pmatrix} \eta_{2\vec{q}}$$

and

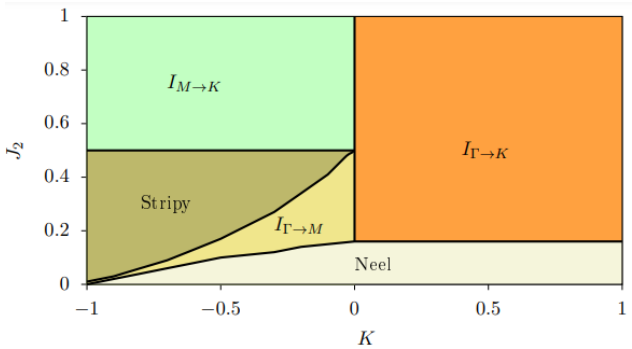

Fig. 2. (Color online) Classical phase diagram of the Kitaev-Heisenberg (***KJ***) model in the $K-J_2$ plane. The solid curves denote the first-order phase boundaries.

$$G_{\vec{q}} = \frac{J_1}{4}\eta_{1\vec{q}}\begin{pmatrix}1&0&0\\0&1&0\\0&0&1\end{pmatrix} + \frac{K}{4}\begin{pmatrix}e_1&0&0\\0&e_2&0\\0&0&1\end{pmatrix} + \frac{\Gamma}{4}\begin{pmatrix}0&1&e_2\\1&0&e_1\\e_2&e_1&0\end{pmatrix}$$

in which

$$e_{1,2} = e^{-i(\pm\frac{1}{2}q_x+\frac{\sqrt{3}}{2}q_y)},$$

$$\eta_{1\vec{q}} = 1 + 2\cos\frac{q_x}{2}e^{-i\frac{\sqrt{3}}{2}q_y},$$

$$\eta_{2\vec{q}} = \cos q_x + 2\cos\frac{1}{2}q_x\cos\frac{\sqrt{3}}{2}q_y$$

To write Eq. (2) in terms of the normalized eigenmodes of H_q leads us to the following simple quadratic form:

$$H = \sum_{\vec{q}}\sum_{\nu=1}^{6}\lambda_{\vec{q}}^{\nu}|\vec{S}_{\vec{q}}^{\nu}|^2 \quad (3)$$

in which λ_q^{ν} presents the eigenvalue of H_q with the $\nu-$th eigenvector as follows

$$H_{\vec{q}}w_{\vec{q}}^{\nu} = \lambda_{\vec{q}}^{\nu}w_{\vec{q}}^{\nu},$$

and the spin structure factor, $\vec{S}_{\vec{q}}^{\prime\nu}$, defined as

$\vec{S}_{\vec{q}}^{\prime\nu} = w_{\vec{q}}^{\nu}\tilde{\vec{S}}_{\vec{q}}$.

In this method, in order to obtain the spin configurations for the set of coupling constants in Eq. (1), we need to find a global minimum λ_0.

Using the weak constrain in the momentum space, the classical energy (Eq. 3) can be reexpressed as:

$$H = N\lambda_0 + \sum_{\vec{q}}\sum_{\nu\neq 0}(\lambda_{\vec{q}}^{\nu}-\lambda_0)|\vec{S}_{\vec{q}}^{\prime\nu}|^2 \quad (4)$$

To minimize this classical energy, the second term in Eq. (4) should be equal to zero due to $(\lambda_q^{\nu}-\lambda_0)>0$. For this purpose, the coefficients $\vec{S}_{\vec{q}}^{\prime\nu}$ with $\nu\neq 0$ need to be eliminated that these generic conditions allow us to realize the spin configurations corresponding to the ground state. It is worth mentioning that if the LT method results in one or more possible spin configurations that fulfill the strong constraint, the physical ground state of the system is found.

3. Results and discussion

Kitaev-Heisenberg *(KJ) model:* To consider the J_1-J_2 antiferromagnetic (AFM) Heisenberg model, we find Neel-type AFM state for $J_2<\frac{1}{6}$. For this case, the minimum of the

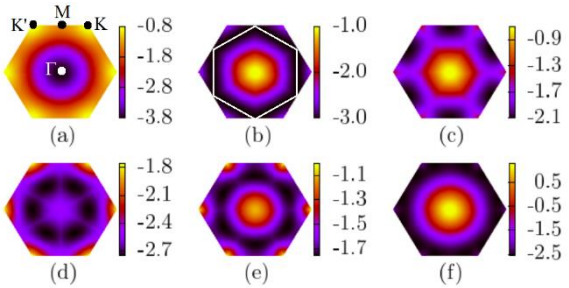

Fig. 3. (Color online) The Fourier-transformed energy of the KJ model within the FBZ for various values of the $J_2$and K terms: (a) $J_2=0.1, K=0$, (b)$J_2=0.23, K=0$ (c) $J_2=0.4, K=-0.5$ (d) $J_2=0.4, K=0.5$, (e) $J_2=-0.2, K=-0.2$, (f) $J_2=0.6, K=-0.5$. The inner white hexagonal in (b) denotes degenerate manifolds of spin spirals in momentum space.

Fourier-transformed energy appears at the AFM point, as shown in Figure 3(a). Beyond $J_2=\frac{1}{6}$, the classical ground state is infinitely degenerate, i.e., the ground-state manifold of the model consists of a set of spiral states characterized by incommensurate wave vectors, so called as classical spin liquid (CSL). The CSL state for $J_2>\frac{1}{6}$ hosts a massive ground-state degeneracy with any wave vector $\vec{q}$ within the FBZ that satisfies the following relation [see Figure 3 (b)]:

$$\cos(\frac{q_x}{2})\cos(\frac{\sqrt{3}}{2}q_y)+\frac{1}{2}\cos(q_x) = \frac{1}{16{J_2}^2}-\frac{3}{4} \quad (5)$$

where these wave vectors form contours in the momentum space around the Γ and K points for $\frac{1}{6}<J_2<\frac{1}{2}$ and $\frac{1}{2}<J_2<1$, respectively [32].

Now, we proceed to present a comprehensive study of the J_1-J_2 model in the presence of the Kitaev term with both ferromagnetic (FM) and AFM interactions. It is noted that A_2IrO_3 [33-35] and $\alpha-RuCl_3$ [37-41] have been suggested to show a large FM Kitaev exchange interaction. However, honeycomb-layered cobaltates $Na_3Co_2SbO_6$ and $Na_2Co_2TeO_6$ are promising new candidates to realize the FM Kitaev interaction [42,43]. Figure 2 illustrates the classical phase diagram of the KJ model in the plane K and J_2. For the case of the AFM Kitaev ($K>0$), the stability region of the Neel order does change, but for $J_2>\frac{1}{6}$ the infinite degeneracy in the ground state can be lifted by the AFM Kitaev interaction and only the magnetic order with an incommensurate wave vector along the $\Gamma\to K$ high-symmetry lines of the FBZ, as shown in Figure 3(d). In this case, the location of the energy minimum closes to the K-point along the $\Gamma\to K$direction with increasing J_2, but the location of the energy minimum does not change with variation of the Kitaev interaction. This incommensurate spiral phase occupies a large part of the phase diagram for $K>0$, labeled as $I_{\Gamma\to K}$ in Figure 2. It is worth mentioning that the ground state degeneracy remains intact for $J_2=\frac{1}{2}$ even for when we consider the AFM Kitaev interaction. For the case of $K<0$, our results indicate that the ground state phase diagram includes four distinct phases [Figure 2]: two commensurate phases (labeled as Neel and Stripy) and two incommensurate orders (called $I_{\Gamma\to M}$ and $I_{M\to K}$). It

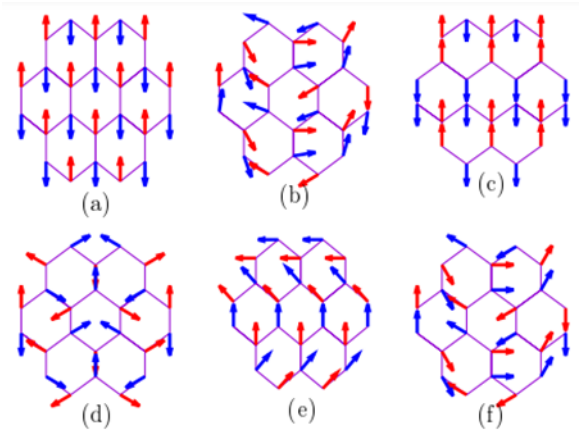

Fig. 4. (Color online) Real-space ordering for some spin configurations in (a) the Neel, (b) the spiral, (c) the stripy, (d) the$I_{\Gamma\to K}$, (e) the$I_{\Gamma\to M}$, and (f) the$I_{M\to K}$phase.

is noted that the stability region of the Neel phase is decreased by increasing $K \to -1$, so that the Neel phase is completely disappeared at $K = -1$. Within this notation, the stripy phase described by $q = M$, as shown in Figure 3(c). In addition, an intermediate incommensurate phase with the energy minimum along the $\Gamma \to M$ [see Figure 3(e)] can be appeared as an intermediate phase between the stripy phase and the commensurate Neel phase, which is called a $I_{\Gamma\to M}$ phase. Our results show that a subtle interplay between the AFM Heisenberg and FM Kitaev exchange interactions plays a decisive role in the stabilizing of the $\Gamma - M$point incommensurate order ($I_{\Gamma\to M}$). It should be mentioned that the phase difference (θ) between the two spins within each unit cell deviates from $\theta = \pi$ in the Neel state boundary to $\theta = 0$ in the stripy phase boundary. For $J_2 > \frac{1}{2}$, the energy minimum is located along the $M \to K$ [see Figure 3(f)], which labeled a $I_{M\to K}$phase. Real-space ordering of spin configurations associated with the classical phase diagram of the KJ model are illustrated in Figure (4).

Kitaev-Heisenberg-Γ ($KJ\Gamma$) model: Here, we mainly focus on the stability of the $I_{\Gamma\to M}$ phase due to the interplay effect between Heisenberg (J) and off-diagonal bond-directional (Γ) exchange interactions. Noted that we consider only $\Gamma > 0$. It is worth mentioning that the off-diagonal Γ interaction is identified to come from the spin-orbit coupling has a positive sign, indicating AFM behavior in $Ba_2Co_2(AsO_4)$ [44]. For the special case with $K = 0$ [Figure 5(a)], our results show that the $I_{\Gamma\to M}$ state appears for $0.2 < J_2 < 0.5$ and all values of $\Gamma \in [0,1]$. To minimize the classical energy, we find that the minimum energy solutions for $J_2 < 0.2$ corresponds to $q = \Gamma$. As a result, the off-diagonal interaction enhances the stability region of the Neel order. For $J_2 > 0.4$, the classical phase diagram of the $KJ\Gamma$ model for given $K = 0$ includes three distinct phases: (i) the $\Gamma - K$point incommensurate order ($I_{\Gamma\to K}$) for $\Gamma < 0.2$, (ii) the $M - K$point incommensurate order ($I_{M\to K}$) for $0.2 < \Gamma < 0.4$, and (iii) the 120°order for $\Gamma > 0.4$. The 120°order described by $q = K$ and $q = K'$for which the two sublattices are completely decoupled. In the presence of the Kitaev interaction, it is found that the interplay effect between the bond-directional exchange interactions favors the stability of a stripy order rather than the $\Gamma - M$ point incommensurate order ($I_{\Gamma\to M}$) in the classical limit, as shown in Figures 5(b-c).

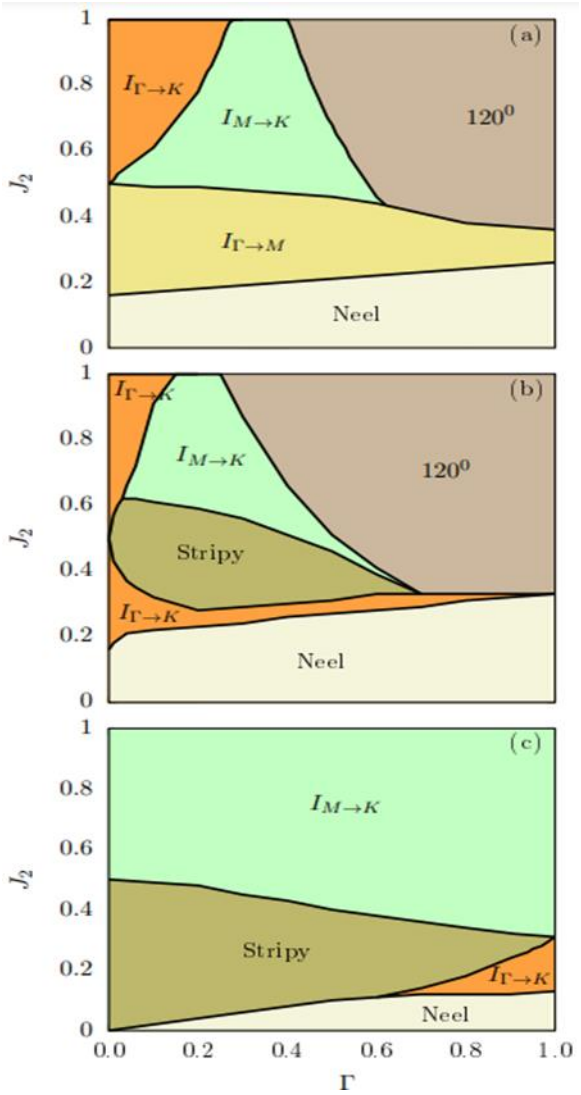

Fig. 5. (Color online) Classical phase diagram of Kitaev-Heisenberg-Γ model in the $\Gamma - J_2$ plane for the various values of the Kitaev term: (a) $K = 0$, (b) $K = 1$, and (c) $K = -1$.

4. Conclusions

In this work, we present a theoretical study of BCAO using the classical LT method. We investigated two theoretical models: the KJ model and the $KJ\Gamma$ model. We indicate that the interplay effect between the Heisenberg and bond-directional exchange interactions play a crucial role in the stability of the $\Gamma - M$ point incommensurate order ($I_{\Gamma\to M}$).

Acknowledgments

M.H.Z. was supported by Grant No. G631021, research deputy of Qom University of Technology.

Conflicts of Interest

The author declares that there is no conflict of interest regarding the publication of this article.

References

[1] Edwards, S. F., and Anderson, P. W., 1975. Theory of spin glasses, *Journal of Physics F: Metal Physics,* 5(5), p.965.

[2] Sherrington D., and Kirkpatrick S., 1975. Solvable Model of a Spin-Glass, *Phys. Rev. Lett.,* 35(26), p.1792.

[3] Anderson, P. W., 1973. Resonating valence bonds: A new kind of insulator, *Materials Research Bulletin,* 8(2), pp. 153-160.

[4] Anderson, P. W., 1987. The resonating valence bond state in la2CuO4 and superconductivity, *Science*, 235(4793) pp.1196-1198.

[5] Balents, L., 2010. Spin liquids in frustrated magnets, *Nature,* 464(7286) pp.199-208.

[6] Zhou, Y., Kanoda, K., and Ng, T.-K., 2017. Quantum spin liquid states, *Rev. Mod. Phys*., 89(2) pp.02500.

[7] Broholm, C., Cava, R. J., Kivelson, S. A., Nocera, D. G., Norman M. R., Senthil, T., 2020. Quantum spin liquids, *Science*, 367(6475), p. eaay0668.

[8] Witczak-Krempa, W., Chen, G., Kim, Y. B., Balents, L., 2014. Correlated quantum phenomena in the strong spin-orbit regime. *Ann. Rev. Conden. Matter Phys*., 5(1) pp.57–82.

[9] Jackeli, G., Khaliullin, G., 2009. Mott insulators in the strong spin-orbit coupling limit: From Heisenberg to a quantum compass and Kitaev models. *Phys. Rev. Lett.,* 102(1), p.017205.

[10] Rau, J. G., Lee, Lee, E. K.-H., Kee, H. Y., 2016. Spin-orbit physics giving rise to novel phases in correlated systems: Iridates and related materials. *Ann. Rev. Condens. Matter Phys. 79(1)* pp.195–221.

[11] Rau, J. G., Lee, E. K.-H., Kee, H. Y., 2014. Generic spin model for the honeycomb iridates beyond the Kitaev limit. *Phys. Rev. Lett.,* 112(7), p.077204.

[12] Xu, G., Xu, Z., Tranquada, J. M., 2013. Absolute cross-section normalization of magnetic neutron scattering data*. Rev. Sci. Inst.*, 84(8), pp.083906.

[13] Plumb, K. W., et al., 2014. α-RuCl3: A spin-orbit assisted Mott insulator on a honeycomb lattice. *Phys. Rev. B,* 90(4), p.041112.

[14] Banerjee, A., et al., 2017. Neutron scattering in the proximate quantum spin liquid α-$RuCl_3$., *Science*, 356(6342), pp.1055–1059.

[15] Takayama, T., et al., 2015. Hyperhoneycomb iridate β-Li2IrO3 as a platform for Kitaev magnetism. *Phys. Rev. Lett.*, 114(7), p.077202.

[16] Gohlke, M., Wachtel, G., Yamaji, Y., Pollmann, F., Kim, Y. B., 2018. Quantum spin liquid signatures in Kitaev-like frustrated magnets. *Phys. Rev. B,* 97(7), p.075126.

[17] Schaffer, R., Bhattacharjee, S., Kim, Y. B., 2012. Quantum phase transition in Heisenberg-Kitaev model. *Phys. Rev. B,* 86(22), p.224417.

[18] Nair, H. S., Brown, J. M., Coldren, E., Hester, G., Gelfand, M. P., Podlesnyak, A., Huang, Q., and Ross, K. A., 2018. Short-range order in the quantum XXZ honeycomb lattice material BaCo2(PO4)2, *Phys. Rev. B,* 97(13), p.134409.

[19] Zhong, R., Gao, T., Ong, N. P., and Cava, R. J., 2020. Weak-field induced nonmagnetic state in a Co-based honeycomb, *Science Advances,* 6(4), p. eaay695.

[20] H. Liu and G. Khaliullin, Pseudospin exchange interactions in d7 cobalt compounds: Possible realization of the Kitaev model, *Phys. Rev. B,* 97 (2018) 014407.

[21] Sano, R., Kato, Y., and Motome, Y., 2018. Kitaev-Heisenberg Hamiltonian for high-spin d7 Mott insulators, *Phys. Rev. B,* 97(1), p.014408.

[22] Regnault, L.-P., Boullier, C., and Lorenzo, J., 2018. Polarized-neutron investigation of magnetic ordering and spin dynamics in BaCo2(AsO4)2 frustrated honeycomb-lattice magnet, *Heliyon,* 4(1), p.e00507.

[23] Tu. C., Dai, D., Zhang, X., Zhao, C., Jin, X., Gao, B., Chen, T., Dai, P., and Li, S., Evidence for gapless quantum spin liquid in a honeycomb lattice, arXiv:2212.07322.

[24] Halloran, T., Desrochers, F., Zhang, E. Z., Chen, T., Chern, L. E., Xu, Z., Winn, B., Graves-Brook, M., Stone. M. B., Kolesnikov, A. I., Qiu, Y., Zhong, R., Cava, R., Kim, Y. B., and Broholm, C., 2023. Geometrical frustration versus Kitaev interactions in $BaCo2(AsO_4)2$*, Proceedings of the National Academy of Sciences,* 120(2), p.e2215509119.

[25] Kitaev A., 2006, Anyons in an exactly solved model and beyond, *Annals of Physics,* 321(1), pp.2111.

[26] Kitaev, A. Y., 2003. Fault-tolerant quantum computation by anyons*, Annals of physics,* 303(1), pp.2-30.

[27] Nayak, C., Simon, S. H., Stern, A., Freedman. M., and Das Sarma, S., 2008, Non-abelian anyons and topological quantum computation, *Rev. Mod. Phys.,* 80(3), p.1083.

[28] Luttinger, J. M., and Tisza, L., 1946. Theory of Dipole Interaction in Crystals, *Phys. Rev*., 70(11-12), p.954.

[29] Litvin, D. B., 1974. The Luttinger-Tisza method, *Physica,* 77(2), pp.205-219.

[30] Rau, J. G., Lee. E. K.-H., and Kee, H.-Y., (2014). Generic Spin Model for the Honeycomb Iridates beyond the Kitaev Limit, *Phys. Rev. Lett.,* 112(7), p.077204.

[31] Rau, J. G. and Kee, H.-Y., Trigonal distortion in the honeycomb iridates: Proximity of zigzag and spiral phases in Na2IrO3, arXiv:1408.4811.

[32] Zare, M.-H., Fazileh, F., Shahbazi, F., 2013. Zero-temperature phase diagram of the classical Kane-Mele Heisenberg model*, Phys. Rev. B,* 87(22), p.224416.

[33] Choi, S. K., Coldea, R., Kolmogorov, A. N., Lancaster, T., Mazin, I. I., Blundell, S. J., Radaelli, P. G., Singh, Y., Gegenwart, P., Choi, K. R., Cheong, S. W., Baker, P. J., Stock. C., and Taylor, J., 2012. Spin Waves and Revised Crystal Structure of Honeycomb Iridate Na2IrO3, *Phys. Rev. Lett.*, 108(12), p.127204.

[34] Hwan, Chun S., Kim, J.-W., Kim, J., Zheng, H., Stoumpos, C. C., Malliakas, C. D., Mitchell, J. F., Mehlawat, K., Singh, Y., Choi, Y., Gog, T., Al-Zein, A., Sala, M. M., Krisch, M., Chaloupka, J., Jackeli, G., Khaliullin, G., and Kim, B. J., 2015. Direct evidence for dominant bond-directional

interactions in a honeycomb lattice iridate Na_2IrO_3, *Nat. Phys.*, 11(6), pp.462–466.

[35] Kimchi, I. and You, Y.-Z., 2011. Kitaev-Heisenberg-J2-J3 model for the iridates A_2IrO_3, *Phys. Rev. B,* 84(18), p.180407.

[36] Kim, J., Chaloupka, J., Singh, Y., Kim, J. W., Kim, B. J., Casa, D., Said., A., Huang, X., and Gog, T., 2020. Dynamic Spin Correlations in the Honeycomb Lattice Na2IrO3 Measured by Resonant Inelastic x-Ray Scattering, *Phys. Rev. X,* 10(2), p.021034.

[37] Plumb, K. W., Clancy, J. P., Sandilands, L. J., Shankar, V. V., Hu, Y. F., Burch, K. S., Kee, H. Y., and Kim, Y. J., 2014. α−RuCl3: A spin-orbit assisted Mott insulator on a honeycomb lattice, *Phys. Rev. B,* 90(4), p.041112(R).

[38] Kubota, Y., Tanaka, H., Ono, T., Narumi, Y., and Kindo, K., 2015. Successive magnetic phase transitions in α−RuC_3: XY-like frustrated magnet on the honeycomb lattice, *Phys. Rev. B,* 91(9), p.094422.

[39] Baek, S. H., Do, S. H., Choi, K. Y., Kwon, Y. S., Wolter, A. U. B., Nishimoto, Van Den Brink, S., J., and Böchner. B., 2017. Successive magnetic phase transitions in α−$RuCl_3$: XY-like frustrated magnet on the honeycomb lattice*, Phys. Rev. Lett.* 119(3), p.037201.

[40] Do, S. H., Park, S. Y., Yoshitake, J., Nasu, J., Motome, Y., Kwon, Y. S., Adroja, D. T., Voneshen, D. J., Kim, K., Jang, T. H., Park, J. H., Choi, K. Y., and Ji, S., 2017. Majorana fermions in the Kitaev quantum spin system α-$RuCl_3$, *Nat. Phys*., 13(11), pp.1079–1084.

[41] Banerjee, A., et al, 2016. Proximate Kitaev quantum spin liquid behaviour in a honeycomb magnet, *Nat. Mater*., 15(7), pp.733–740.

[42] Kaib, David A. S., Winter, Stephen M., and Valentí, Roser, 2019. Kitaev honeycomb models in magnetic fields: Dynamical response and dual models, *Phys. Rev. B*, 100(14), p.144445.

[43] Kim, Chaebin, et al, 2022. Antiferromagnetic Kitaev interaction in Jeff = 1/2 cobalt honeycomb materials Na3Co2SbO6 and Na2Co2TeO6, *Phys.: Condens. Matter*, 34(4), p.045802.

[44] Liu, Xiaoyu, and Kee, Hae-Young, 2023. Non-Kitaev versus Kitaev honeycomb cobaltates. Phys. Rev. B. 107(9), p.054420.